Paper: ASAT-15-192-ST

15th International Conference on
AEROSPACE SCIENCES & AVIATION TECHNOLOGY,
ASAT - 15 – May 28 - 30, 2013, Email: asat@mtc.edu.eg ,
Military Technical College, Kobry Elkobbah, Cairo, Egypt,
Tel: +(202) 24025292 –24036138, Fax: +(202) 22621908

Design Improvement of Composite Pressure Vessel Structure

W. M. Mahdy*, H. Taher†, E. E. El-Soaly‡

Abstract: This paper presents a proposed approach for improving the design of a composite pressure vessel (CPV) under internal pressure. Thin shell theory, membrane theory, classical lamination theory and Tsai–Wu failure criterion are carefully integrated into an efficient mathematical model. The mathematical model is successfully combined with an in-house developed algorithm that is used to improve the design of any given CPV. Case results show that the proposed approach successfully improved the design of a composite pressure vessel relative to the base design made from steel and also relative to a conventional CPV design approach.

Keywords: Composite materials, pressure vessels, structural design, design improvement

1. Introduction

Fiber reinforced polymer (FRP) composite materials with their higher specific strength and stiffness characteristics will result in reduction of weight of the structure. So, CPV_s are an important type of high-pressure container that is widely used in the commercial and aerospace industries.

The design objective is to make the pressure vessel as lightweight as possible; within the bounds of technology, cost, structural strength, handling and storage. When the metal alloys are replaced by composite materials, in general the structure's mass will be reduced by 20–30% [1]. Additionally, Laminate patterns and ply buildup in a part can be tailored to give the required mechanical properties in various directions. Design of CPV_s is very complicated and requires careful consideration of factors. Material properties, fiber orientation, stacking sequence are considered the most important parameters in designing of Composite pressure vessels. It was found that most of the design and analysis of CPV_s are based on thin-walled theory; which outer diameter is less than 1.1 times its inner diameter [2]. Roylance [3] used netting analysis for filament wound pressure vessels which assumed that all loads are supported by the fibers only, neglecting any contribution by the matrix and any interaction between the fibers. He noted that the optimum winding angle for filament-wound pressure vessels is 54.74°.

The classical lamination theory (CLT) is utilized to determine the stresses and strains at any position of laminates subjected to force and/or moment resultants. On the other hand, the Tsai–Wu failure criterion used to predict the first-ply failure load. Liang [4] used CLT as optimization core for domes of rocket motor case. He also used Tsai-Wu failure criterion to

* Egyptian Armed Forces, Egypt; walid_lolo2020@yahoo.com ;
† Egyptian Armed Forces, Egypt, heltaher@gmail.com ;
‡ Professor, High Institute of Technology of 10th Ramadan, October branch, Egypt

assess the first ply failure. Chapelle, D. [5] provided an exact solution for stresses and strains on the cylindrical section of the vessel under thermo-mechanical static loading based on CLT and on Tsai Hill's criterion. Tsai-Wu failure criterion was used to evaluate the fracture behavior of composite layers [6, 7]. Additionally, Tsai-Wu failure criterion was used to determine the laminate thickness distributions [8].

However, one disadvantage of the composite materials is dull design processes [9]. So, it was important to do a computer program in order to reduce the calculating time of designing the CPV. MATLAB, a numerical computing package, was used as a basis for the programs as it is more than sufficient to handle the numerous matrix computations [9]. This program is improved to achieve the minimum thickness of the CPV those can safely withstand the applied load given the available composite material.

2. Mechanics of Composite Materials

The unit cell structure of a composite material is called a lamina. A lamina is a flat (sometimes curved as in shell) arrangement of unidirectional or woven fibers in a supporting matrix. When several laminas are stacked together, this structure is called a laminate. A laminate is a stack of laminas with various orientations of principal material directions in the lamina. A laminate's layers are usually bound together by the same matrix material that is used in the lamina. Strain-stress relations for plane stress orthotropic lamina can be described as follows [10]:

$$\begin{Bmatrix} \varepsilon_1 \\ \varepsilon_2 \\ \gamma_{12} \end{Bmatrix} = \begin{bmatrix} S_{11} & S_{12} & 0 \\ S_{12} & S_{22} & 0 \\ 0 & 0 & S_{66} \end{bmatrix} \begin{Bmatrix} \sigma_1 \\ \sigma_2 \\ \tau_{12} \end{Bmatrix} \tag{1}$$

where $[S]$ is the compliance matrix and its elements are:

$$S_{11} = \frac{1}{E_1} \quad , \quad S_{12} = -\frac{\upsilon_{12}}{E_1} = -\frac{\upsilon_{21}}{E_2} \quad , \quad S_{22} = \frac{1}{E_2} \quad , \quad S_{66} = \frac{1}{G_{12}}$$

where $E_{1,2}$ are Young's modulus in directions 1 and 2; G_{12} is the shear modulus in the 1-2 plane; $\upsilon_{12,21}$ are Poisson's ratios in the 1-2 and 2-1planes.

Stress-strain relations for a lamina with arbitrary orientation are:

$$\{\sigma\}_x = \begin{bmatrix} m^2 & n^2 & 2mn \\ n^2 & m^2 & -2mn \\ -mn & mn & m^2-n^2 \end{bmatrix}^{-1} [Q] \begin{bmatrix} m^2 & n^2 & mn \\ n^2 & m^2 & -mn \\ -2mn & 2mn & m^2-n^2 \end{bmatrix} \{\varepsilon\}_x \tag{2}$$

where $[Q]$ is the stiffness matrix and it is equal to the inverse of $[S]$; m and n are cosine and sine of angle (θ) between global (x,y,z) and material coordinates (1,2,3), respectively (as shown in Figure 1. For simplicity equation (2) can be written as follows:

$$\{\sigma\}_x = \left[\bar{Q}\right]\{\varepsilon\}_x \tag{3}$$

where $\left[\bar{Q}\right]$ is called the transformed stiffness matrix.

The stress strain relation in equation (3) can now be used in finding stresses and strains under external applied loads using the CLT [11]. The theory assumes that for a laminate consisting of orthotropic laminas, a line that passes perpendicularly to the mid-surface remains straight and perpendicular after deformation as shown in Figure 2. The mid-surface strains and curvatures in the global coordinate can be used to find stresses of the number k lamina as follows:

$$\{\sigma\}^k = \left[\bar{Q}\right]^k \{\varepsilon\}_o + z\left[\bar{Q}\right]^k \{\kappa\}_x \tag{4}$$

where $\{\varepsilon\}_o$ and $\{\kappa\}_x$ are mid-surface strain and curvature, respectively.

The in-plane forces (N_x, N_y, N_{xy}) and moments (M_x, M_y, M_{xy}) per unit length are defined as the through-thickness integrals of the planer stress in the laminate as shown in Figure 3.

Figure 3 and can be expressed as follows:

$$\begin{aligned} \{N\} &= \int_{-h/2}^{h/2} \{\sigma\}\, dz \\ \{M\} &= \int_{-h/2}^{h/2} \{\sigma\}\, z dz \end{aligned} \tag{5}$$

Substitution of (4) into (5) yields the following matrix relations that relate the force and moment resultants to the mid-surface strains and curvatures,

$$\begin{aligned} \{N\} &= \int_{-h/2}^{h/2} \left[\bar{Q}\right]^k \{\varepsilon^o\}\, dz + \int_{-h/2}^{h/2} \left[\bar{Q}\right]^k \{\kappa\}\, z dz \\ \{M\} &= \int_{-h/2}^{h/2} \left[\bar{Q}\right]^k \{\varepsilon^o\}\, z dz + \int_{-h/2}^{h/2} \left[\bar{Q}\right]^k \{\kappa\}\, z^2 dz \end{aligned} \tag{6}$$

The integral over laminate thickness can be replaced by a summation of integrals over the individual layer's thickness, where $\{\varepsilon^o\}$ and $\{\kappa\}$ are independent of z. Thus,

$$\begin{aligned} \{N\} &= \sum_{k=1}^{N} \left(\int_{z_{k-1}}^{z_k} \left[\bar{Q}\right]^k dz \right) \{\varepsilon^o\} + \sum_{k=1}^{N} \left(\int_{z_{k-1}}^{z_k} \left[\bar{Q}\right]^k z dz \right) \{\kappa\} \\ \{M\} &= \sum_{k=1}^{N} \left(\int_{z_{k-1}}^{z_k} \left[\bar{Q}\right]^k z dz \right) \{\varepsilon^o\} + \sum_{k=1}^{N} \left(\int_{z_{k-1}}^{z_k} \left[\bar{Q}\right]^k z^2 dz \right) \{\kappa\} \end{aligned} \tag{7}$$

Or more simply

$$\begin{Bmatrix} N \\ M \end{Bmatrix} = \begin{bmatrix} A & B \\ B & D \end{bmatrix} \begin{Bmatrix} \varepsilon^o \\ \kappa \end{Bmatrix} \tag{8}$$

where $[A]$ is called the extensional stiffness, $[B]$ is the bending-extensional coupling stiffness and $[D]$ is the bending stiffness; and each can be defined as follows:

$$\begin{aligned} [A] &= \sum_{k=1}^{N} \left[\bar{Q}\right]^k (z_k - z_{k-1}) \\ [B] &= \frac{1}{2} \sum_{k=1}^{N} \left[\bar{Q}\right]^k (z_k^2 - z_{k-1}^2) \\ [D] &= \frac{1}{3} \sum_{k=1}^{N} \left[\bar{Q}\right]^k (z_k^3 - z_{k-1}^3) \end{aligned} \tag{9}$$

Combining the above equations gives the most general expression for stress at any z-location in a laminate with given forces and moments as:

$$\{\sigma\}^k = [\bar{Q}]^k \left\{ \left([A]^{-1} + [A]^{-1}[B][W][B][A]^{-1} - z[W][B][A]^{-1} \right)[N] - \left([A]^{-1}[B] - z[I] \right)[W][M] \right\} \quad (10)$$

where [I] is an identity matrix and [W] is

$$[W] = \left([D] - [B][A]^{-1}[B] \right)^{-1}$$

The presence of nonzero elements in the coupling matrix $[B]$ indicates that the application of in-plane traction will lead to a curvature or warping of the plate, conversely an applied bending moment will also generate an extensional strain. In structural design, these effects are usually undesirable; however they can be avoided by making the laminate symmetric about the mid-plane. A laminate is called symmetric when for each layer on one side of a mid-plane there is a corresponding layer at an equal distance from the mid-plane on the other side with identical thickness, orientation, and properties. The laminate is symmetric in both geometry and material properties. The stress at any z-location in a symmetric laminate with given forces and moments can be given as:

$$\{\sigma\}^k = \left[\bar{Q}\right]^k [A]^{-1}[N] + z\left[\bar{Q}\right]^k [D]^{-1}[M] \quad (11)$$

In a case of pressure vessel subjected to internal pressure, the stresses in cylindrical part is

$$\{N\} = \left[\frac{pr}{2},\ pr,\ 0 \right]^T \quad (12)$$

where p and r are the internal pressure and inner radius, respectively [12].

3. Failure Criterion

A failure criterion is now required to evaluate and differentiate different composite designs according to their structural efficiency. There are various failure theories such as maximum stress, maximum strain, Tsai-Hill, and Tsai-Wu. There are large differences between the results of maximum stress, maximum strain, and experimental results. The results of Tsai-Hill and Tsai-Wu are found in good agreement with the experimental results. Tsai-Wu is more accurate than Tsai-Hill failure theory, because the interaction between the stress components and Tsai-Wu theory does distinguish between the tensile and compressive strengths [13].

The second-order tensor polynomial criterion as proposed by [14] is considered here. The criterion assumes that there exists a failure surface in the stress-space in the following scalar form:

$$f(\sigma_k) = F_i\sigma_i + F_{ij}\sigma_i\sigma_j = 1 \quad (13)$$

where the contracted notation is used; and i, j, k = 1,...6; F_i and F_{ij} are strength tensors of the second and fourth rank, respectively.

By assuming that F_i and F_{ij} are symmetric tensors, equation (13) in expanded form is

$$
\begin{aligned}
&F_1\sigma_1 + F_2\sigma_2 + F_3\sigma_3 + F_4\sigma_4 + F_5\sigma_5 + F_6\sigma_6 \\
&\quad + F_{11}\sigma_1^2 + 2F_{12}\sigma_1\sigma_2 + 2F_{13}\sigma_1\sigma_3 + 2F_{14}\sigma_1\sigma_4 + 2F_{15}\sigma_1\sigma_5 + 2F_{16}\sigma_1\sigma_6 \\
&\quad + F_{22}\sigma_2^2 + 2F_{23}\sigma_2\sigma_3 + 2F_{24}\sigma_2\sigma_4 + 2F_{25}\sigma_2\sigma_5 + 2F_{26}\sigma_2\sigma_6 \\
&\quad + F_{33}\sigma_3^2 + 2F_{34}\sigma_3\sigma_4 + 2F_{35}\sigma_3\sigma_5 + 2F_{36}\sigma_3\sigma_6 \\
&\quad + F_{44}\sigma_4^2 + 2F_{45}\sigma_4\sigma_5 + 2F_{46}\sigma_4\sigma_6 \\
&\quad + F_{55}\sigma_5^2 + 2F_{56}\sigma_5\sigma_6 \\
&\quad + F_{66}\sigma_6^2 = 1
\end{aligned}
\tag{14}
$$

Other simplification of equation (14) can be effected through recognition that the shear terms $F_4 = F_5 = F_6 = 0$ and the normal/shear coupling terms $F_{14} = F_{15} = F_{16} = F_{24} = F_{25} = F_{26} = F_{34} = F_{35} = F_{36} = F_{45} = F_{46} = F_{56} = 0$.

Thus, the reduced form of the scalar function $f(\sigma_k)$ for orthotropic material is

$$
\begin{aligned}
&F_1\sigma_1 + F_2\sigma_2 + F_3\sigma_3 + F_{11}\sigma_1^2 + F_{22}\sigma_2^2 + F_{33}\sigma_3^2 + F_{44}\sigma_4^2 + F_{55}\sigma_5^2 + F_{66}\sigma_6^2 \\
&2F_{12}\sigma_1\sigma_2 + 2F_{13}\sigma_1\sigma_3 + 2F_{23}\sigma_2\sigma_3 = 1
\end{aligned}
\tag{15}
$$

The expanded form of this theory is stated as [15]

$$
F_1\sigma_1 + F_2\sigma_2 + F_{11}\sigma_1^2 + F_{22}\sigma_2^2 + F_{66}\tau_{12}^2 + 2F_{12}\sigma_1\sigma_2 \geq 1 \tag{16}
$$

where F_1, F_2, and so on are called the strength coefficients and are given by [15]

$$
\begin{aligned}
F_1 &= \frac{1}{\sigma_1^T} + \frac{1}{\sigma_1^C} \quad , \quad F_{11} = -\frac{1}{\sigma_1^T\sigma_1^C} \\
F_2 &= \frac{1}{\sigma_2^T} + \frac{1}{\sigma_2^C} \quad , \quad F_{22} = -\frac{1}{\sigma_2^T\sigma_2^C} \\
F_{12} &= -\frac{1}{2}\sqrt{F_{11}F_{22}} \quad , \quad F_{66} = \frac{1}{\left(\tau_{12}^F\right)^2}
\end{aligned}
\tag{17}
$$

where σ_1^T is the tensile strength in the longitudinal direction, σ_2^T is the Tensile strength in the transverse direction, σ_1^C is the compression strength in longitudinal direction, σ_2^C is the compression strength in the transverse direction, and τ_{12}^F is the in-plane shear strength.

Tsai-Wu failure criterion can be determined whether a lamina has failed or not. However, this does not give the information about how much the load can be increased if the lamina is safe or how much the load should be decreased if the lamina has failed. The definition of strength ratio (SR) is helpful here. The strength ratio is defined as the ratio between the maximum load which can be applied and load applied [13]. Each stress component of equation (16) was multiplied by the SR as:

$$
\left(F_1\sigma_1 + F_2\sigma_2\right)SR + \left(F_{11}\sigma_1^2 + F_{22}\sigma_2^2 + F_{66}\tau_{12}^2 + 2F_{12}\sigma_1\sigma_2\right)SR^2 \geq 1 \tag{18}
$$

The criterion for SR is that it can only be positive. If SR is < 1, then failure occurs because it means that the loading needs to decrease to avoid failure. A value SR =1 implies that the composite structure is perfectly suited for the applied loading conditions. If SR >1, then the lamina is more safe and we have to increasing the applied stress by a factor of SR or decreasing the lamina's thickness (mass of the structure) for the same stress with in the safety limits.

4. Proposed Approach

The proposed approach to improve the design of a composite pressure vessel is described in this section. The approach employs a mathematical model for calculating the minimum number of composite layers those can safely withstand the applied load given the available composite material. This approach improves on the conventional approach which only ensures that the laminate will safely withstand the applied load regardless of it is overdesigned (non-optimal) or not. The mathematical model is represented by a flow chart in Figure 4. The mathematical model starts with given input: composite material properties, stacking sequence of one laminate, applied load, and required dimensions and safety factor.

Then focusing on this laminate, the [A], [B], and [D] matrices are calculated and used to estimate the minimum strength ratio (SR) over all laminate's plies. Since the laminate will obviously not be able to withstand the applied load, SR will be less than one, which means composite failure. However, calculating the reciprocal of SR and multiplying it by the value of the required safety factor will give us a rough estimate of the number of multiple laminates required to increase the loading capacity until SR is higher than one and is equal to the value of the safety factor. This rough estimate of laminates number will give an over designed composite and the program will now start to iterate to decrease unnecessary laminates until the minimum value of SR over all laminate's plies is equal to the value of the required safety factor. The program then stops and uses the density of composite material to calculate the required material mass per unit area; hence this value can be compared with the mass of a base design of a pressure vessel made from steel. A comparison between the normalized weights of different patterns is shown in Figure 5.

5. Results and Discussion

Before presenting the design improvement results, the verification of the mathematical model is firstly presented. The mathematical model has been verified against the published results of example 4.3 in page 335 in Ref. [13]. In this example, a composite laminate is made from [0°/30°/–45°] graphite epoxy laminate where each lamina is 5 mm thick. The material properties are given in Table 3. The laminate is subjected to 1000 N/m in the x and y global coordinates.

The local stresses and strains are calculated using the mathematical model and are compared with the published results presented in Ref. [13] as presented in Table 1. It is clear that there is a complete agreement between both results.

In the next step, the mathematical model is also verified in order to ensure that failure criterion calculations are correct. The mathematical model is verified using the published results of example 5.3 in page 381 in Ref. [13]. In this example, a composite laminate is made from $[0/9\bar{0}]_s$ graphite epoxy laminate where each lamina is 5 mm thick. The laminate is subjected to 1 N/m in the x global coordinate parallel to the fibers in the 0 ply. Strength ratios are calculated using the mathematical model and are compared with the published results in Ref. [13] as presented in Table 2. Again, there is a complete agreement between both results. The mathematical model is verified and can be used in developing the proposed approach.

A case study of a composite pressure vessel is used to demonstrate the proposed approach. A vessel of 540 mm diameter made from Kevlar 49/ Epoxy 934 [16] subjected to 120 bars internal pressure is considered. It is assumed that all plies have equal 0.125 mm thickness.

The objective now is starting with an initial design find an optimum design that sustain the applied load with the required safety at the minimum possible material weight. In order to obtain meaningful results, all results are compared with a base design of a pressure vessel made from AISI 4140 steel which its material properties are given in Table 4.

Different laminate stacking sequences are used for the composite pressure vessel and the values of mass per unit area for conventional composite design, i.e. overdesigned where strength ratio is higher than the required safety factor. In other words, an overdesign has unnecessary laminates those have been eliminated using the proposed approach. Values of mass per unit area [kg/m^2] for conventional and improved composite designs along with a base steel design are all given in Table 5.

It should be noted that only symmetric composite laminates have been used in order to avoid unwanted warping under axial loading which is achieved by ensuring that the coupling [B] matrix is zeroed. The results are discussed in the following sections.

It is interesting to note that lowest values are achieved at an angle ply stacking sequence of $[54.74/-54.74]_s$. This can be explained by the fact that this is the optimum stacking sequence for a composite pressure vessel, which can be considered the final design of a conventional design approach. This specific angle allows for uniform tension in all fibers, a situation known as isotensoid. An analytical derivation is neatly explained in Ref. [17]. However, although this is the optimum stacking sequence, the proposed approach has even successfully improved it and managed to decrease the required mass even more as shown in the grayed row in Table 5.

Another interesting note is that all composite stacking sequences gave even much higher masses per unit area except for $[54.74/-57.44]_s$ and $[0/90/90]_s$. The $[54.74/-57.44]_s$ is the optimum (best) stacking sequence where the $[0/90/90]_s$ (row 3 in Table 5) is the natural intuitive selection for fiber orientation. This is because in a pressure vessel, hoop stresses (σ_y) are twice the values as axial stresses (σ_x), hence it is only logical to put two times fibers in the hoop (90°) direction as in the axial (0°) direction.

The highest mass per unit area has been obtained with a composite with all fibers oriented in the axial (0°) direction (row 1 in Table 5). This is because aligning all fibers along the axial direction meant that fibers were able to provide only their lowest contribution to the hoop (90°) direction, subsequently much more fibers were required in order to give strength capacity in the hoop direction.

Aligning all fibers along the hoop direction (row 2 in Table 5) gave lower mass per unit area values than the previous unidirectional case. This is because in the $[90/90/90]_s$ case all fibers are now aligned along the higher stress (hoop direction). On the other hand, it can be noted that aligning fibers in other angle ply arrangement at [30/60] and [±45] will also lead to sub-optimal results where the [±45] is better than the [30/60] since the former arrangement distributes the load carrying fibers equally in the axial and hoop directions.

6. Conclusion

In this paper, a proposed approach for improving the design of pressure vessels made from composite materials has been presented. A mathematical model has been developed for modeling composite pressure vessels under loading and this model has been solved using MATLAB and the mathematical model has been validated using published data. An algorithm has been developed in order to improve the design of a composite pressure vessel relative to a base design made from steel. The proposed approach managed to successfully improve the design of a composite pressure vessel by reducing 37% of its weight compared to only 20% reduction of a conventional approach.

7. References

[1] V. V. Vasiliev and E. V. Morozov, *Advanced mechanics of composite materials*: Elsevier Science Limited, 2007.

[2] A. Onder, O. Sayman, T. Dogan, and N. Tarakcioglu, "Burst failure load of composite pressure vessels," *Composite structures,* vol. 89, pp. 159-166, 2009.

[3] D. K. ROYLANCE, "Nettting analysis for filament - wound pressure vessels," pp. 1-9, 1976.

[4] C. C. Liang, H. W. Chen, and C. H. Wang, "Optimum design of dome contour for filament-wound composite pressure vessels based on a shape factor," *Composite structures,* vol. 58, pp. 469-482, 2002.

[5] D. Chapelle and D. Perreux, "Optimal design of a Type 3 hydrogen vessel: Part I—Analytic modelling of the cylindrical section," *International Journal of Hydrogen Energy,* vol. 31, pp. 627-638, 2006.

[6] J. L. Pelletier and S. S. Vel, "Multi-objective optimization of fiber reinforced composite laminates for strength, stiffness and minimal mass," *Computers & Structures,* vol. 84, pp. 2065-2080, 2006.

[7] A. Hocine, D. Chapelle, M. Boubakar, A. Benamar, and A. Bezazi, "Experimental and analytical investigation of the cylindrical part of a metallic vessel reinforced by filament winding while submitted to internal pressure," *International journal of pressure vessels and piping,* vol. 86, pp. 649-655, 2009.

[8] L. Zu, S. Koussios, and A. Beukers, "Design of filament–wound domes based on continuum theory and non-geodesic roving trajectories," *Composites Part A: Applied Science and Manufacturing,* vol. 41, pp. 1312-1320, 2010.

[9] A. Ramsaroop and K. Kanny, "Using MATLAB to Design and Analyse Composite Lami-nates," *Engineering,* vol. 2, pp. 904-916, 2010.

[10] C. T. Herakovich, "Mechanics of fibrous composites," *New York: John Wiley & Sons, Inc, 1998.*, 1998.

[11] J. N. Reddy, *Mechanics of laminated composite plates and shells: theory and analysis*: CRC, 2003.

[12] E. J. Hearn, *An introduction to the mechanics of elastic and plastic deformation of solids and structural materials*: Butterworth-Heinemann, 1997.

[13] A. K. Kaw, *Mechanics of composite materials* vol. 29: CRC, 2005.

[14] S. W. Tsai and E. M. Wu, "A general theory of strength for anisotropic materials," *Journal of composite materials,* vol. 5, pp. 58-80, 1971.

[15] P. Xu, J. Zheng, and P. Liu, "Finite element analysis of burst pressure of composite hydrogen storage vessels," *Materials & Design,* vol. 30, pp. 2295-2301, 2009.

[16] S. T. Peters, *Handbook of Composites,* 2nd ed.: Chapman & Hall, 1998.

[17] S. V. H. Daniel Gay, Stephen W. Tsai, *Composite materials design and applications*: CRC PRESS, 2003.

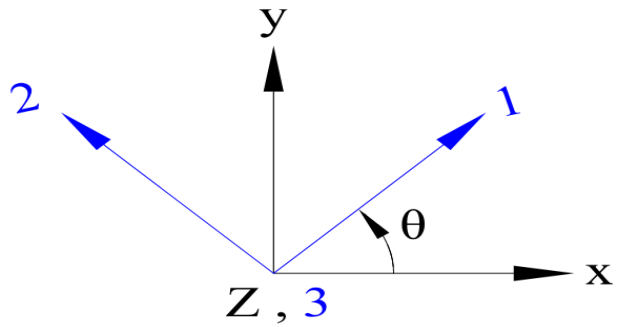

Figure 1 Global and local coordinates of a lamina

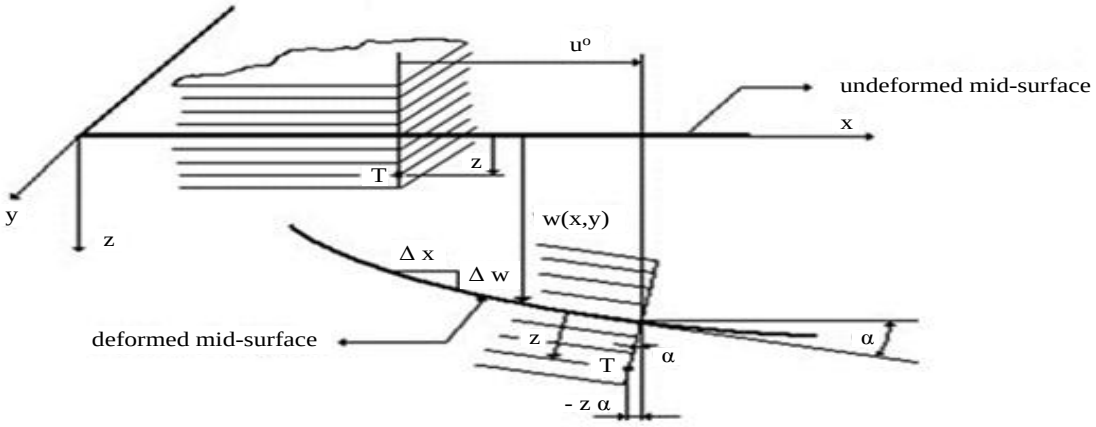

Figure 2 A schematic drawing of a laminate before and after loading

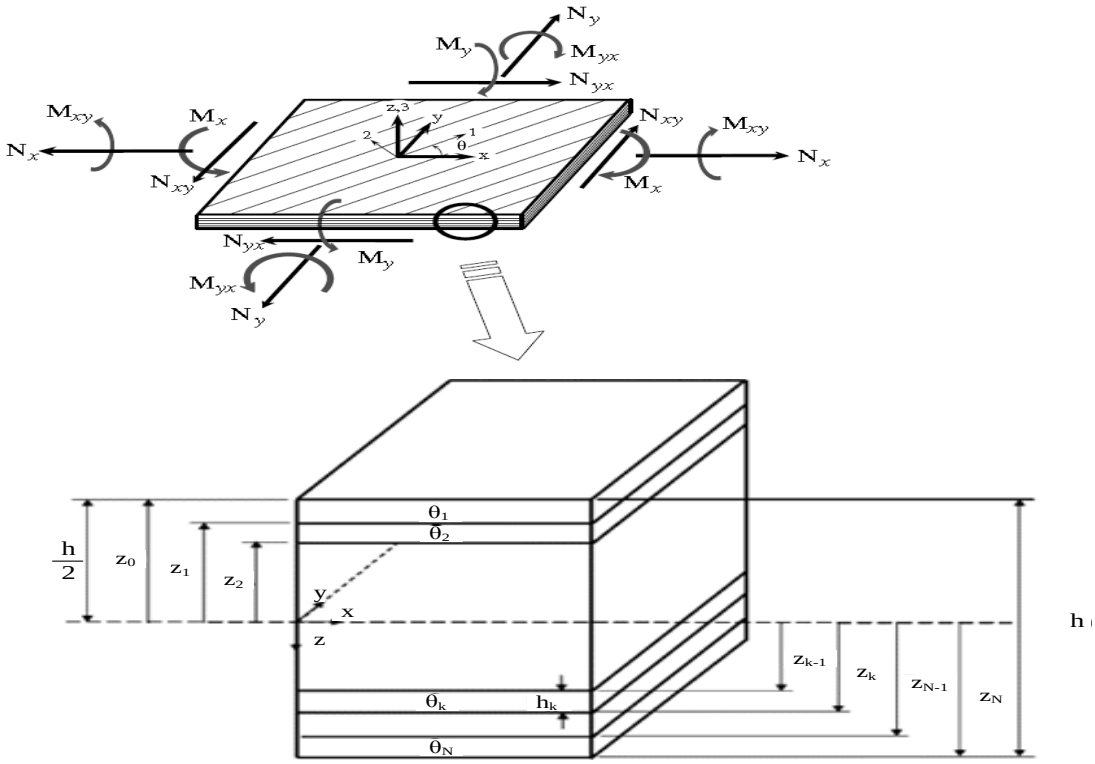

Figure 3 Representation of a composite laminate subjected to external force and moment

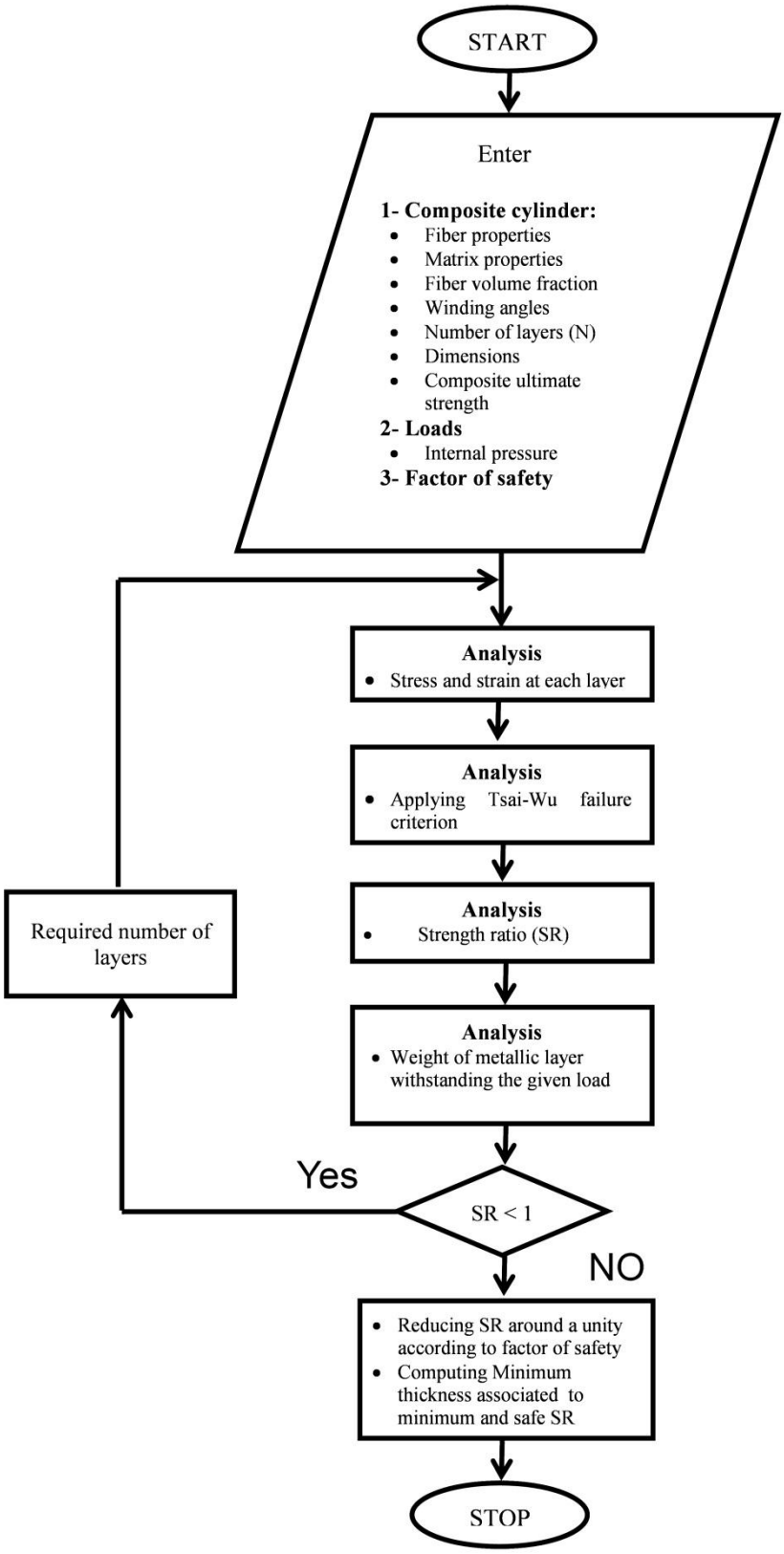

Figure 4 Flow chart of the proposed approach

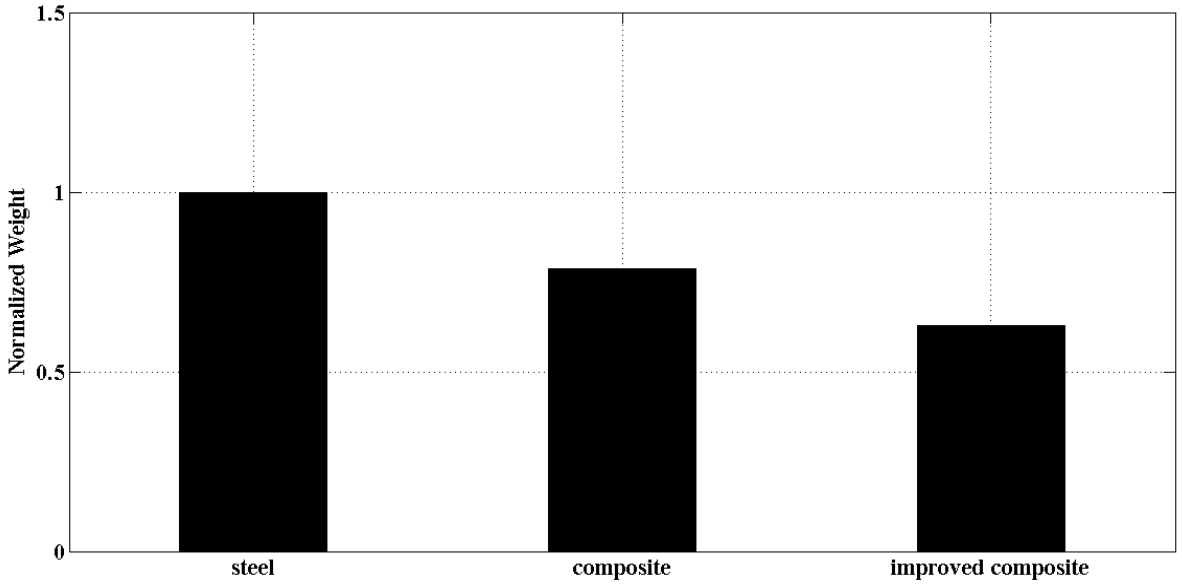

Figure 5 Comparison between the normalized weights of different patterns

Table 1 Model verification results of stresses and strains for each layer

Stacking Sequence		Ref. [13]		Mathematical model	
		Local Stress (pa)	Local Strain (m/m)	Local Stress (pa)	Local Strain (m/m)
0°	Top	$\begin{Bmatrix}3.351\\6.188\\-2.750\end{Bmatrix}\times10^{4}$	$\begin{Bmatrix}0.08944\\5.955\\-3.836\end{Bmatrix}\times10^{-6}$	$\begin{Bmatrix}3.3513\\6.1875\\-2.7504\end{Bmatrix}\times10^{4}$	$\begin{Bmatrix}0.0894\\5.9555\\-3.8359\end{Bmatrix}\times10^{-6}$
	Bottom	$\begin{Bmatrix}5.577\\4.531\\-1.280\end{Bmatrix}\times10^{4}$	$\begin{Bmatrix}0.238\\4.313\\-1.785\end{Bmatrix}\times10^{-6}$	$\begin{Bmatrix}5.5767\\4.5312\\-1.2800\end{Bmatrix}\times10^{4}$	$\begin{Bmatrix}0.238\\4.313\\-1.7852\end{Bmatrix}\times10^{-6}$
30°	Top	$\begin{Bmatrix}9.973\\4.348\\1.890\end{Bmatrix}\times10^{4}$	$\begin{Bmatrix}0.4837\\4.067\\2.636\end{Bmatrix}\times10^{-6}$	$\begin{Bmatrix}9.9730\\4.3482\\1.8903\end{Bmatrix}\times10^{4}$	$\begin{Bmatrix}0.4837\\4.0672\\2.6364\end{Bmatrix}\times10^{-6}$
	Bottom	$\begin{Bmatrix}20.07\\2.364\\1.513\end{Bmatrix}\times10^{4}$	$\begin{Bmatrix}1.073\\1.985\\2.111\end{Bmatrix}\times10^{-6}$	$\begin{Bmatrix}20.075\\2.364\\1.513\end{Bmatrix}\times10^{4}$	$\begin{Bmatrix}1.0725\\1.9845\\2.1106\end{Bmatrix}\times10^{-6}$
-45°	Top	$\begin{Bmatrix}25.86\\2.123\\-1.638\end{Bmatrix}\times10^{4}$	$\begin{Bmatrix}1.396\\1.661\\-2.284\end{Bmatrix}\times10^{-6}$	$\begin{Bmatrix}25.858\\2.123\\-1.638\end{Bmatrix}\times10^{4}$	$\begin{Bmatrix}1.3958\\1.6613\\-2.2839\end{Bmatrix}\times10^{-6}$
	Bottom	$\begin{Bmatrix}-6.285\\1.898\\-0.3533\end{Bmatrix}\times10^{4}$	$\begin{Bmatrix}-0.3766\\1.940\\-0.4928\end{Bmatrix}\times10^{-6}$	$\begin{Bmatrix}-6.2848\\1.8977\\-0.3533\end{Bmatrix}\times10^{4}$	$\begin{Bmatrix}-0.3766\\1.9397\\-0.4928\end{Bmatrix}\times10^{-6}$

Table 2 Model verification results of strength ratios for each layer

Stacking Sequence		Ref. [13]	Mathematical model
		SR	SR
0°	Top	1.339×10^{7}	1.3394×10^{7}
	Bottom	1.339×10^{7}	1.3394×10^{7}
90°	Top	0.7277×10^{7}	0.7277×10^{7}
	Bottom	0.7277×10^{7}	0.7277×10^{7}
0°	Top	1.339×10^{7}	1.3394×10^{7}
	Bottom	1.339×10^{7}	1.3394×10^{7}

Table 3 Mechanical properties of kevlar/epoxy [16]

Material Properties						Material Limits				
E_1 (GPa)	E_2 (GPa)	G_{12} (GPa)	υ_{12}	V_f	ρ (kg/m^3)	σ_1^T (MPa)	σ_1^C (MPa)	σ_2^T (MPa)	σ_2^C (MPa)	τ_{12}^F (MPa)
72	5	2	0.41	0.60	1350	1151	281	12	134	443

Table 4 Mechanical properties of AISI 4140 [15]

Property	Value
E [GPa]	207
Y	0.27
σ_Y [MPa]	680
σ_U [MPa]	850
Density [kg/m^3]	7850

Table 5 Results of mass per unit area [kg/m^2] for conventional and improved composite and steel designs for different laminate stacking sequence

Stacking sequence	Conventional composite design	Improved composite design	Base steel design
$[0/0/0]_s$	724.5127	534.6506	36.5246
$[90/90/90]_s$	274.6406	209.7900	
$[0/90/90]_s$	45.0056	36.0506	
$[54.74/-54.74]_s$	30.1806	23.6725	
$[0/30/60]_s$	390.1556	295.7189	
$[0/60/30]_s$	390.1556	295.7189	
$[0/45/-45]_s$	189.2756	145.8127	
$[0/-45/45]_s$	189.2756	145.8127	